XIV International Conference on Computational Plasticity. Fundamentals and Applications
COMPLAS XIV
E. Oñate, D.R.J. Owen, D. Peric & M. Chiumenti (Eds)

MULTIPHYSICAL FAILURE PROCESSES IN CONCRETE: A CONSISTENT MULTISCALE HOMOGENIZATION PROCEDURE

Felipe Lopez Rivarola[a], **Nicolás Agustín Labanda**[abc], **and Guillermo J. Etse**[ac]

[a]Universidad de Buenos Aires. Facultad de Ingeniería. LMNI-INTECIN (UBA-CONICET), Buenos Aires, Argentina.
e-mail: getse@herrera.unt.edu.ar, web page: http://laboratorios.fi.uba.ar/lame/

[b] SRK consulting and Universidad Nacional de Tucumán, Argentina.
Email: nlabanda@srk.com.ar, web page : http://latam.srk.com/en and http://facet.unt.edu.ar

[c]CONICET - Universidad Nacional de Tucumán, Faculty of Exact Science and Engineering.

Key words: Multiphysical phenomena, poromechanics, multi-scale, failure.

Abstract. Durability and strength capabilities of concrete materials are vastly affected by the combined action of temperature and mechanical loading, which give rise to multiphysical failure processes. Such a phenomenon involves complex cracking, degradation and transport mechanisms on different scale lengths of concrete mixtures which, in turn, depend on the particular properties of the different constituents. Thus, the macroscopic observation of relevant concrete mechanical features such as strength, ductility and durability are the result of several different properties, processes and mechanisms which are not only coupled but moreover, depend on multiple scales. Particularly, regarding the pore pressure and thermal actions, most of the degradation processes in concrete are controlled by the heterogeneities of the microscopic scale. In the case of the mechanical actions both the micro and mesoscales play a relevant role. In this context, multiphysical failure processes in cementitious material-based mixtures like concrete can only and fully be understood and accurately described when considering its multiscale and multiconstituent features. In the realm of the theoretical and computational solid mechanics many relevant proposals were made to model the complex and coupled thermo-hydromechanical response behavior of concrete. Most of them are related to macroscopic formulations which account for the different mechanisms and transport phenomena through empirical, dissipative, poromechanical theories. Moreover, although relevant progress was made regarding the formulation of multiscale theories and approaches, none of the existing proposals deal with multiphysical failure processes in concrete. It should be said in this sense that, among the different multiscale approaches for material modeling proposed so far, those based on computational homogenization methods have demonstrated to be the most effective ones due to the involved versatility and accuracy. In this work a thermodynamically consistent semi-concurrent multiscale approach is formulated for modeling the

thermo-poro-plastic failure behavior of concrete materials. A discrete approach is considered to represent the RVE material response. After formulating the fundamental equations describing the proposed homogenizations of the thermodynamical variables, the constitutive models for both the skeleton and porous phases are described. Then, numerical analyses are presented to demonstrate the predictive capabilities of the proposed thermodynamically consistent multiscale homogenization procedure for thermo-mechanical failure processes in concrete mixtures.

1 INTRODUCTION

A thermo-poro-mechanical multi-scale problem to model concrete degradation is presented in this paper and schematically represented in Figure 1. The multi-scale model is stated within the semi-concurrent formulations [1] where the strain tensor $\boldsymbol{\varepsilon}$, the temperature θ and it gradient $\nabla\theta$ is transferred from the coarse scale to the fine scale. The mortar in the micro-scale (or representative volume element **RVE**) is considered a porous media. Biot's poromechanics theory is considered for the mortar simulation, while the aggregate is simulated as a simple elastic material. After solving the boundary value problem in the fine-scale the macro-stress $\boldsymbol{\sigma}(x,t)$, the macro-heat flux $\boldsymbol{q}(x,t)$ and the macro-pore pressure $p(x,t)$ are obtained.

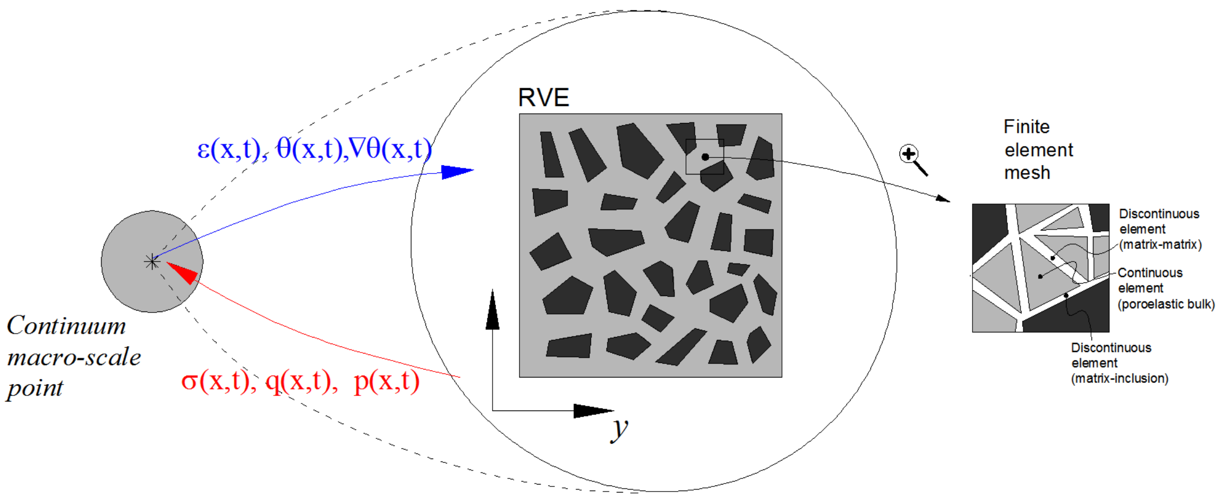

Figure 1: Schematic representation of the proposed multi-scale procedure.

The paper is organized as follow: the themo-poro-mechanic problem in the coarse scale is stated in Section 2. Multi-scale equations are given in Section 3. Fine scale constitutive modelling and some thermodynamics aspects are discussed in Section 4. A numerical example is presented in Section 5 and finally, some conclusions are drawn in Section 6.

2 Thermo-poro-mechanical problem in the coarse scale

In the following section, the equilibrium equations for a thermo-poro-mechanics with undrained hydraulic conditions are presented. It is important to note that all variables with sub-index μ, are those acting in the fine scale.

The thermal problem can be expressed as: *Given a thermal source f, find $\theta \in \Theta$ such that the heat flux $\boldsymbol{q}$ fulfil*

$$\int_{\Omega} \boldsymbol{q} \cdot \nabla_{\boldsymbol{x}} \delta\theta \; d\Omega = \int_{\Omega} f \delta\theta \; d\Omega, \qquad \forall \delta\theta \in \Theta. \tag{1}$$

The poro-mechanical problem can be expressed as: *Given a temperature field θ that satisfied* (1) *and a load in the Neumann boundary $\boldsymbol{f}$, find $\boldsymbol{u} \in \mathscr{U}$ such that the stress field $\boldsymbol{\sigma}$ fulfil*

$$\int_{\Omega} \boldsymbol{\sigma}\left(\boldsymbol{u}_{\mu}, p_{\mu}, \theta_{\mu}\right) \cdot \nabla^{s}_{\boldsymbol{x}} \delta\boldsymbol{u} \; d\Omega = \int_{\Gamma} \boldsymbol{f} \cdot \delta\boldsymbol{u} \; d\Gamma, \qquad \forall \delta\boldsymbol{u} \in \mathscr{U} \tag{2}$$

where

$$\Theta = \left\{\theta \in \boldsymbol{H}^{1}\left(\Omega\right) : essential\ boundary\ conditions\right\} \tag{3}$$

$$\mathscr{U} = \left\{\delta\boldsymbol{u} \in \boldsymbol{H}^{1}\left(\Omega\right) : essential\ boundary\ conditions\right\} \tag{4}$$

In equation 1 it can be seen that the macro stress tensor $\boldsymbol{\sigma}\left(\boldsymbol{u}_{\mu}, p_{\mu}, \theta_{\mu}\right)$ depends on three micro scale variables: the micro-scale displacement $\boldsymbol{u}_{\mu}$, the micro-scale pore pressure p_{μ} and the micro-scale temperature θ_{μ}.

3 Multi-scale framework

Given a point $\boldsymbol{x} \in \Omega$ in the macro scale and being $\boldsymbol{y} \in \Omega_{\mu}$ the coordinate system in the **RVE**, the following scale bridging equations can be formulated.

3.1 Thermal problem

- Axiom 1 - Kinematical admissibility

The following scale transition equation for the temperature gradient is considered

$$\nabla_{\boldsymbol{x}}\theta = \frac{1}{|\Omega_{\mu}|} \int_{\Omega_{\mu}} \nabla_{\boldsymbol{y}}\theta_{\mu} \; d\Omega_{\mu} \;\Rightarrow\; \nabla_{\boldsymbol{x}}\theta = \frac{1}{|\Omega_{\mu}|} \int_{\partial\Omega_{\mu}} \theta_{\mu}\boldsymbol{n} \; d\partial\Omega_{\mu}, \tag{5}$$

being n the external normal of the **RVE** boundary $\partial\Omega_{\mu}$. In the same way, the temperature compatibility between scales is defined

$$\theta = \frac{1}{|\Omega_{\mu}|} \int_{\Omega_{\mu}} \theta_{\mu} \; d\Omega_{\mu}. \tag{6}$$

The insertion of the macro-scale temperature gradient $\nabla_{\boldsymbol{x}}\theta$ in the micro-scale temperature field θ_{μ}, is considered as

$$\theta_{\mu}\left(\boldsymbol{y}\right) = \theta + \nabla_{\boldsymbol{x}}\theta \cdot \left(\boldsymbol{y} - \boldsymbol{y}_{0}\right) + \tilde{\theta}_{\mu}\left(\boldsymbol{y}\right) \;\Rightarrow\; \nabla_{\boldsymbol{y}}\theta_{\mu}\left(\boldsymbol{y}\right) = \nabla_{\boldsymbol{x}}\theta + \nabla_{\boldsymbol{y}}\tilde{\theta}_{\mu} \tag{7}$$

with

$$\boldsymbol{y}_0 = \frac{1}{|\Omega_\mu|} \int_{\Omega_\mu} \boldsymbol{y} \; d\Omega_\mu. \tag{8}$$

Introducing equation (7) in (6) the following constraint over the temperature fluctuation field is obtained

$$\int_{\Omega_\mu} \tilde{\theta}_\mu \; d\Omega_\mu = 0 \tag{9}$$

Finally, the space of kinematically admissible fluctuations in the microscopic temperature field are

$$\tilde{\Theta}_\mu = \left\{ \theta_\mu \in \boldsymbol{H}^1 \left(\Omega_\mu\right) : \int_{\Omega_\mu} \theta_\mu \; d\Omega_\mu = 0, \; \int_{\partial\Omega_\mu} \theta_\mu \boldsymbol{n} \; d\partial\Omega_\mu = 0 \right\} \tag{10}$$

- Axiom 2 - Multi-scale virtual principle

The thermal multi-scale virtual principle can be written as

$$\boldsymbol{q} \cdot \nabla_{\boldsymbol{x}} \delta\theta = \frac{1}{|\Omega_\mu|} \int_{\Omega_\mu} \boldsymbol{q}_\mu \left(\theta_\mu\right) \cdot \nabla_{\boldsymbol{y}} \delta\theta_\mu \; d\Omega_\mu, \quad \forall \; \delta\theta_\mu \; \nabla_{\boldsymbol{x}} \delta\theta \; admissible \tag{11}$$

- Consequence 1 - Thermal equilibrium problem in the **RVE**

Considering $\nabla_{\boldsymbol{x}} \delta\theta = 0$ in equation 11, the thermal equilibrium equation in the microscale is obtained

$$\frac{1}{|\Omega_\mu|} \int_{\Omega_\mu} \boldsymbol{q}_\mu \left(\theta_\mu\right) \cdot \nabla_{\boldsymbol{y}} \delta\tilde{\theta}_\mu \; d\Omega_\mu = 0, \quad \forall \; \delta\tilde{\theta}_\mu \in \tilde{\Theta}_\mu \tag{12}$$

- Consequence 2 - Homogenization operator for thermal flux

Considering $\delta\tilde{\theta}_\mu = 0$ in equation 11, the homogenization operator for the thermal flux is obtained

$$\boldsymbol{q} = \frac{1}{|\Omega_\mu|} \int_{\Omega_\mu} \boldsymbol{q}_\mu \left(\theta_\mu\right) \; d\Omega_\mu. \tag{13}$$

A Fourier law for materials in the fine scale will be considered

$$\boldsymbol{q}_\mu \left(\theta_\mu\right) = -\boldsymbol{K}_\mu \nabla_{\boldsymbol{y}} \theta_\mu. \tag{14}$$

3.2 Thermo-poro-mechanical problem

- Axiom 1 - Kinematical admissibility

For the scale transition equations a fractured **RVE** domain noted as Γ_μ with normal $\boldsymbol{n}_\mu$ is considered

$$\boldsymbol{\varepsilon} = \frac{1}{|\Omega_\mu|} \left[\int_{\Omega_\mu} \nabla^s_{\boldsymbol{y}} \boldsymbol{u}_\mu \; d\Omega_\mu + \int_{\Gamma_\mu} [\![\boldsymbol{u}_\mu]\!] \otimes^s \boldsymbol{n}_\mu d\Gamma_\mu \right]. \tag{15}$$

Applying Green's theorem to equation 15, the following equations is obtained

$$\varepsilon = \frac{1}{|\Omega_\mu|}\int_{\partial\Omega_\mu} \boldsymbol{u}_\mu \otimes^s \boldsymbol{n}\; d\partial\Omega_\mu. \tag{16}$$

The insertion of the macro-scale strain tensor ε in the **RVE** kinematics, is defined as

$$\boldsymbol{u}_\mu = \boldsymbol{u} + \varepsilon\left(\boldsymbol{y} - \boldsymbol{y}_0\right) + \tilde{\boldsymbol{u}}_\mu, \;\Rightarrow\; \nabla^s_{\boldsymbol{y}}\boldsymbol{u}_\mu = \varepsilon + \nabla^s_{\boldsymbol{y}}\tilde{\boldsymbol{u}}_\mu. \tag{17}$$

Finally, the space of kinematically admissible displacement fluctuations are

$$\tilde{\mathscr{U}}_\mu = \left\{\boldsymbol{u} \in \boldsymbol{H}^1(\Omega) : \int_{\Omega_\mu} \boldsymbol{u}\; d\Omega_\mu = 0,\; \int_{\partial\Omega_\mu} \boldsymbol{u}\otimes^s \boldsymbol{n}\; d\partial\Omega_\mu = 0\right\} \tag{18}$$

- Axiom 2 - Multi-scale virtual principle for poro-mechanical problems

The multi-scale virtual principle considering a poro-mechanic material in the **RVE** with undrained hydraulic conditions, can be expressed as

$$\boldsymbol{\sigma}\cdot\nabla^s_{\boldsymbol{x}}\delta\boldsymbol{u} = \frac{1}{|\Omega_\mu|}\int_{\Omega_\mu} \boldsymbol{\sigma}_\mu\left(\boldsymbol{u}_\mu, p_\mu, \theta_\mu\right)\cdot\nabla^s_{\boldsymbol{y}}\delta\boldsymbol{u}_\mu\; d\Omega_\mu + \int_{\Gamma_\mu} \boldsymbol{t}_\mu\cdot[\![\delta\boldsymbol{u}_\mu]\!]d\Gamma_\mu,\;\; \forall\delta\boldsymbol{u}\;\delta\boldsymbol{u}_\mu\; admissible, \tag{19}$$

where the last term is the contribution of the activated cohesive elements in the multi-scale virtual power.

- Consequence 1 - Micro-mechanical equilibrium problem

Considering $\nabla^s_{\boldsymbol{x}}\delta\boldsymbol{u} = 0$ in equation 19, the micro-scale equilibrium equation is obtained

$$\int_{\Omega_\mu} \boldsymbol{\sigma}_\mu\left(\boldsymbol{u}_\mu, p_\mu, \theta_\mu\right)\cdot\nabla^s_{\boldsymbol{y}}\delta\tilde{\boldsymbol{u}}_\mu\; d\Omega_\mu + \int_{\Gamma_\mu} \boldsymbol{t}_\mu\cdot[\![\delta\boldsymbol{u}_\mu]\!]d\Gamma_\mu = 0,\;\; \forall\delta\tilde{\boldsymbol{u}}_\mu \in \tilde{\mathscr{U}}_\mu \tag{20}$$

- Consequence 2 - Homogenization operator for the stress tensor

Considering $\delta\tilde{\boldsymbol{u}}_\mu = 0$ in equation 19, the homogenization operator for the stress tensor is obtained

$$\boldsymbol{\sigma} = \frac{1}{|\Omega_\mu|}\int_{\Omega_\mu} \boldsymbol{\sigma}_\mu\left(\boldsymbol{u}_\mu, p_\mu, \theta_\mu\right)\; d\Omega_\mu. \tag{21}$$

4 Helmholtz free energy in the RVE

Following Ref. [2], the energetic consistency in the micro-scale is stated considering the Helmholtz free energy as follows

$$\boldsymbol{\psi}_\mu\left(\nabla^s_{\boldsymbol{y}}\boldsymbol{u}_\mu, p_\mu, \theta_\mu\right) = \boldsymbol{\psi}^B_\mu\left(\nabla^s_{\boldsymbol{y}}\boldsymbol{u}_\mu, p_\mu, \theta_\mu\right) + \boldsymbol{\psi}^F_\mu\left(\delta_\mu\right), \tag{22}$$

where ψ_μ^B is the Helmholtz free energy for the bulk phase and ψ_μ^F is the Helmholtz free energy for the fractured phase, defined as [3, 4]

$$\begin{aligned}\psi_\mu^B\left(\nabla_{\boldsymbol{y}}^s \boldsymbol{u}_\mu, p_\mu, \theta_\mu\right) = & \frac{1}{2}\,\mathbb{C}_\mu\left(\nabla_{\boldsymbol{y}}^s \boldsymbol{u}_\mu\right)\cdot\left(\nabla_{\boldsymbol{y}}^s \boldsymbol{u}_\mu\right) - \boldsymbol{B}_\mu\left(\nabla_{\boldsymbol{y}}^s \boldsymbol{u}_\mu\right)\theta_\mu + \\ & + \frac{1}{2} M_w b_w^2\left(tr\left(\nabla_{\boldsymbol{y}}^s \boldsymbol{u}_\mu\right) - \frac{\zeta_w}{b_w}\right)^2 + \frac{1}{2}\left(-\frac{\mathscr{C}}{T_0} + M_w\alpha_w^2\right)\theta_\mu^2 + \\ & - M_w b_w\left(tr\left(\nabla_{\boldsymbol{y}}^s \boldsymbol{u}_\mu\right) - \frac{\zeta_w}{b_w}\right)\alpha_w\theta_\mu + \chi_\mu\rho_\mu\zeta_w,\end{aligned} \tag{23}$$

and

$$\psi_\mu^F\left(\delta_\mu\right) = \begin{cases} G_c\frac{\delta_\mu}{\delta_c}\left(2 - \frac{\delta_\mu}{\delta_c}\right), & if \quad \delta_\mu \leq \delta_c \\ G_c, & if \quad \delta_\mu > \delta_c \end{cases}, \quad with \quad \delta_\mu = \sqrt{[\![\boldsymbol{u}_\mu]\!]\cdot[\![\boldsymbol{u}_\mu]\!]}\;. \tag{24}$$

The coefficients needed to calibrate the porous media in the model are: b_w the Biot coefficient, M_w the Biot modulus, $\zeta_w = \phi_w S_w$ the water volumetric fraction being ϕ_w water porosity and S_w the degree of saturation, α_w coefficient of thermal expansion, $\mathscr{C}$ volumetric heat capacity and T_0 the reference temperature. The skeleton part is calibrated using the elastic material operator

$$\mathbb{C}_\mu = \frac{E_\mu}{1-\nu_\mu^2}\left[\left(1-\nu_\mu\right)\mathbb{I} + \nu_\mu\left(\boldsymbol{I}\otimes\boldsymbol{I}\right)\right] \tag{25}$$

and the tensor of thermomechanical expansion of the skeleton

$$\boldsymbol{B}_\mu = \frac{\alpha_\mu E_\mu}{1-\nu_\mu^2}\left[1 + \nu_\mu\left(tr\boldsymbol{I} - 1\right)\right]\boldsymbol{I} \tag{26}$$

Considering Coleman's relations, from equation 22 the following relation can be obtained

$$\begin{aligned}\sigma_\mu\left(\nabla_{\boldsymbol{y}}^s \boldsymbol{u}_\mu, p_\mu, \theta_\mu\right) = \frac{\partial\psi_\mu}{\partial\nabla_{\boldsymbol{y}}^s \boldsymbol{u}_\mu} = & \;\mathbb{C}_\mu\left(\nabla_{\boldsymbol{y}}^s \boldsymbol{u}_\mu\right) - \boldsymbol{B}_\mu\theta_\mu + \\ & + M_w b_w\left[b_w\left(tr\left(\nabla_{\boldsymbol{y}}^s \boldsymbol{u}_\mu\right) - \zeta_w - \alpha_w\theta_\mu\right)\boldsymbol{I}\right]\end{aligned} \tag{27}$$

or expressed in term of the pore pressure

$$\sigma_\mu\left(\nabla_{\boldsymbol{y}}^s \boldsymbol{u}_\mu, p_\mu, \theta_\mu\right) = \mathbb{C}_\mu\left(\nabla_{\boldsymbol{y}}^s \boldsymbol{u}_\mu\right) - \boldsymbol{B}_\mu\theta_\mu + b_w p_\mu\boldsymbol{I} \tag{28}$$

It is interesting to note that combining equation 28 with 21 the homogenization of the total stress in the macro scale is the result of the homogenization of the effective stress in the micro-scale plus the homogenization of the porous pressure in the micro-scale

$$\boldsymbol{\sigma} = \boldsymbol{\sigma}' + \boldsymbol{p}, \tag{29}$$

being the effective stress

$$\begin{aligned}\boldsymbol{\sigma}' = & \left(\frac{1}{|\Omega_\mu|}\int_{\Omega_\mu}\mathbb{C}_\mu \; d\Omega_\mu\right)\boldsymbol{\varepsilon} + \frac{1}{|\Omega_\mu|}\int_{\Omega_\mu}\mathbb{C}_\mu \; \left(\nabla^s_{\boldsymbol{y}}\tilde{\boldsymbol{u}}_\mu\right) \; d\Omega_\mu - \left(\frac{1}{|\Omega_\mu|}\int_{\Omega_\mu}\boldsymbol{B}_\mu \; d\Omega_\mu\right)\theta + \\ & - \left(\frac{1}{|\Omega_\mu|}\int_{\Omega_\mu}\boldsymbol{B}_\mu \otimes (\boldsymbol{y}-\boldsymbol{y}_0) \; d\Omega_\mu\right)\cdot\nabla^s_{\boldsymbol{x}}\theta - \frac{1}{|\Omega_\mu|}\int_{\Omega_\mu}\boldsymbol{B}_\mu\tilde{\theta}_\mu \; d\Omega_\mu\end{aligned} \tag{30}$$

and the pore pressure

$$\boldsymbol{p} = \frac{1}{|\Omega_\mu|}\int_{\Omega_\mu} b_w p_\mu \; d\Omega_\mu \boldsymbol{I}, \quad with \;\; p_\mu = M_w\left[b_w\left(tr\left(\nabla^s_{\boldsymbol{y}}\boldsymbol{u}_\mu\right) - \zeta_w - \alpha_w\theta_\mu\right)\right]. \tag{31}$$

The homogenized constitutive tensor $\mathbb{C}$ retains the classical structure. To compute tensors $\boldsymbol{B}$ and $\boldsymbol{G}$ two extra assumption are considered: a temperature invariant Biot coefficient and a constant fluid mass. The first order thermomechanical contribution to the macroscopic stress tensor is

$$-\frac{\partial\boldsymbol{\sigma}}{\partial\theta} = \boldsymbol{B} = \overline{\boldsymbol{B}} + \tilde{\boldsymbol{B}} + \boldsymbol{B}^p, \tag{32}$$

where

$$\overline{\boldsymbol{B}} = \frac{1}{|\Omega_\mu|}\int_{\Omega_\mu}\boldsymbol{B}_\mu \; d\Omega_\mu, \quad \tilde{\boldsymbol{B}} = -\frac{1}{|\Omega_\mu|}\int_{\Omega_\mu}\mathbb{C}_\mu \; \left(\nabla^s_{\boldsymbol{y}}\frac{\partial\tilde{\boldsymbol{u}}_\mu}{\partial\theta}\right) \; d\Omega_\mu, \tag{33}$$

while the contribution of the pore pressure can be stated as

$$\boldsymbol{B}^p = \frac{1}{|\Omega_\mu|}\int_{\Omega_\mu} b_w\frac{\partial p_\mu}{\partial\theta} \; d\Omega_\mu\boldsymbol{I}, \quad with \;\; \frac{\partial p_\mu}{\partial\theta} = M_w\left[b_w\left(tr\left(\nabla^s_{\boldsymbol{y}}\frac{\partial\tilde{\boldsymbol{u}}_\mu}{\partial\theta}\right) - \alpha_w\right)\right]. \tag{34}$$

In the same way, the second order thermomechanical contribution to the macroscopic stress can be stated as

$$-\frac{\partial\boldsymbol{\sigma}}{\partial\nabla^s_x\theta} = \boldsymbol{G} = \overline{\boldsymbol{G}} + \tilde{\boldsymbol{G}} + \boldsymbol{G}^p, \tag{35}$$

where

$$\overline{\boldsymbol{G}} = \frac{1}{|\Omega_\mu|}\int_{\Omega_\mu}\boldsymbol{B}_\mu\otimes(\boldsymbol{y}-\boldsymbol{y}_0) \; d\Omega_\mu, \tag{36}$$

$$\begin{aligned}\tilde{\boldsymbol{G}} = -\Bigg[&\frac{1}{|\Omega_\mu|}\int_{\Omega_\mu}\left(\mathbb{C}_\mu\left(\nabla^s_x\left[\frac{\partial\tilde{\boldsymbol{u}}_\mu}{\partial\nabla^s_x\theta}\right]_k\right)\right)_{ij} \; d\Omega_\mu + \\ & -\frac{1}{|\Omega_\mu|}\int_{\Omega_\mu}(\boldsymbol{B}_\mu)_{ij}\left[\frac{\partial\tilde{\theta}_\mu}{\partial\nabla^s_x\theta}\right]_k \; d\Omega_\mu\Bigg](\boldsymbol{e}_i\otimes\boldsymbol{e}_j\otimes\boldsymbol{e}_k),\end{aligned} \tag{37}$$

while the contribution of the pore pressure is

$$\boldsymbol{G}^p = \frac{1}{|\Omega_\mu|}\int_{\Omega_\mu} b_w\frac{\partial p_\mu}{\partial\nabla^s_x\theta} \; d\Omega_\mu\boldsymbol{I}, \tag{38}$$

with

$$\frac{\partial p_\mu}{\partial \nabla_x^s \theta} = M_w \left[b_w \left(tr \left(\nabla_{\boldsymbol{y}}^s \frac{\partial \tilde{\boldsymbol{u}}_\mu}{\partial \nabla_x^s \theta} \right) - \alpha_w \left(\boldsymbol{y} - \boldsymbol{y}_0 + \frac{\partial \tilde{\theta}_\mu}{\partial \nabla_x^s \theta} \right) \right) \right]. \tag{39}$$

The homogenized macroscopic stress can then be calculated as

$$\boldsymbol{\sigma} = \mathbb{C}\boldsymbol{\varepsilon} - \boldsymbol{B}\theta - \boldsymbol{G}\nabla_x^s \theta. \tag{40}$$

5 Numerical examples

Some numerical examples are presented in this section, considering an uncoupled scheme solution for the thermo-poro-mechanical problem. The proposed **RVE** for the analysis in concrete is presented in Figure 2.

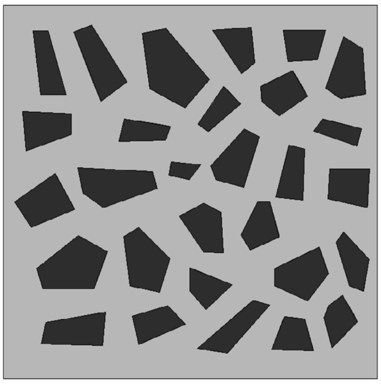

Figure 2: Proposed **RVE** for thermo-poromechanical analysis.

5.1 Multi-scale thermal problem

The considered thermal conductivity tensor for cement mortar and aggregates are

$$\boldsymbol{K}_\mu^{mortar} = \begin{bmatrix} 0.7 & 0 \\ 0 & 0.7 \end{bmatrix} \frac{W}{m\,°C}, \qquad \boldsymbol{K}_\mu^{aggreg} = \begin{bmatrix} 3.0 & 0 \\ 0 & 3.0 \end{bmatrix} \frac{W}{m\,°C}. \tag{41}$$

Using the homogenization procedure presented for the thermal problem, the following homogenized thermal conductivity tensors for different sub-spaces of equation 10 are obtained $\left(\text{in } \frac{W}{m\,°C}\right)$

$$\begin{aligned} \boldsymbol{K}^{Taylor} &= \begin{bmatrix} 1.3696 & 0 \\ 0 & 1.3696 \end{bmatrix}, \qquad & \boldsymbol{K}^{Linear} &= \begin{bmatrix} 1.079 & 0.0024854 \\ 0.0024854 & 1.0622 \end{bmatrix}, \\ \boldsymbol{K}^{Periodic} &= \begin{bmatrix} 1.0754 & 0.0023161 \\ 0.0023161 & 1.0573 \end{bmatrix}, \qquad & \boldsymbol{K}^{Traction} &= \begin{bmatrix} 1.0724 & 0.0023531 \\ 0.0023531 & 1.0549 \end{bmatrix}. \end{aligned} \tag{42}$$

Considering a temperature gradient of $\nabla_x^s \theta = [1; 0]$ and the homogenized tensors, the macroscopic flux vectors in each case are

$$\begin{aligned} \boldsymbol{q}^{Taylor} &= \begin{bmatrix} 1.3696 \\ 0 \end{bmatrix} \frac{W}{m^2}, & \boldsymbol{q}^{Linear} &= \begin{bmatrix} 1.079 \\ 0.0024854 \end{bmatrix} \frac{W}{m^2}, \\ \boldsymbol{q}^{Periodic} &= \begin{bmatrix} 1.0754 \\ 0.0023161 \end{bmatrix} \frac{W}{m^2}, & \boldsymbol{q}^{Traction} &= \begin{bmatrix} 1.0724 \\ 0.0023531 \end{bmatrix} \frac{W}{m^2}. \end{aligned} \tag{43}$$

It can be seen that the macroscopic thermal flux vectors presented in the last equations have a different direction compared with the introduced macroscopic temperature gradient due to the anisotropy induced by the stochastic nature of the aggregate distribution. The Taylor (classical mixture theory) sub-space is the only one not capable of recognizing this effect, as it does not consider the heterogeneous geometrical conformation of the micro-structure.

Considering the minimally restricted space, or uniform traction space, and introducing a macroscopic temperature of $\theta = 100°C$, figure 3 shows the temperature distribution within the considered **RVE** for different values in $\nabla_x^s \theta$. It can be seen that the average value in the microscopic temperature field θ_μ is the macroscopic introduced temperature.

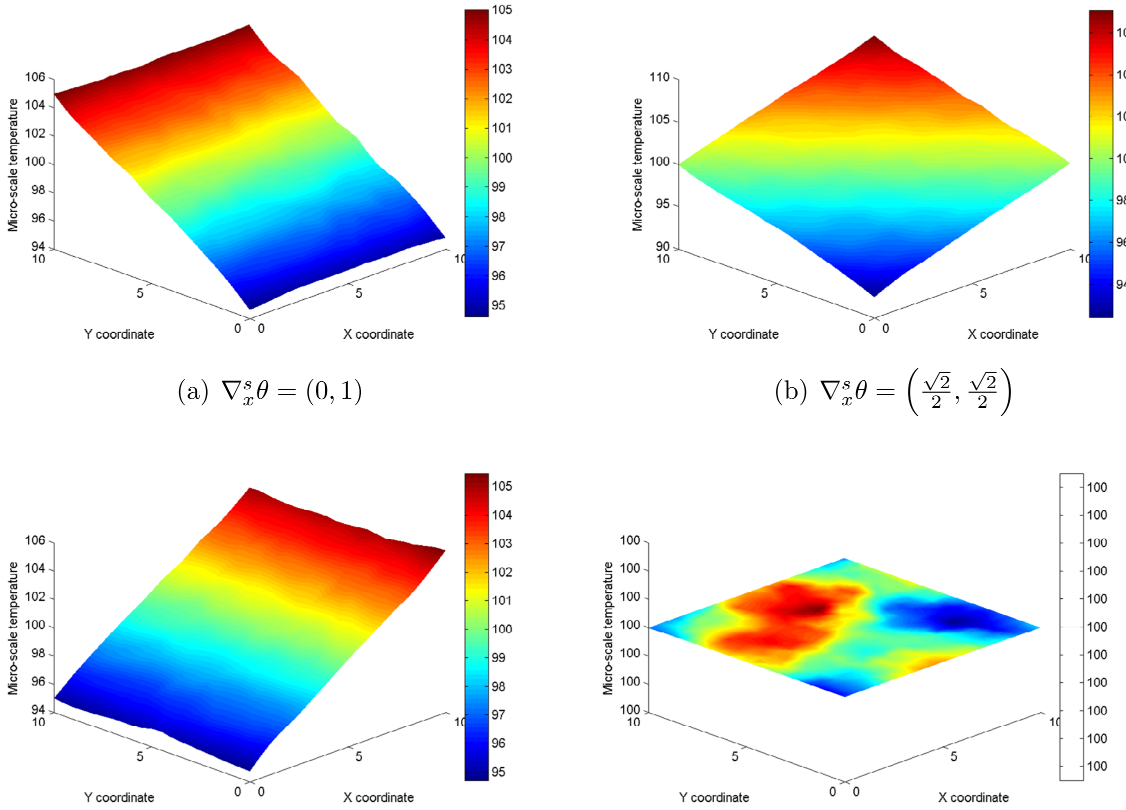

(a) $\nabla_x^s \theta = (0, 1)$

(b) $\nabla_x^s \theta = \left(\frac{\sqrt{2}}{2}, \frac{\sqrt{2}}{2}\right)$

(c) $\nabla_x^s \theta = (1, 0)$

(d) $\nabla_x^s \theta = (0, 0)$

Figure 3: Temperature distribution within the **RVE**.

5.2 Multi-scale thermo-mechanical problem

In order to study the thermo-mechanical problem, a constant thermal distribution in concordance with a temperature gradient $\nabla_x^s \theta = (0, 0)$ is considered. The material parameters used to characterize the components of the micro-scale are presented in Table 1. The macro-scale temperature is increased and then returned to the initial temperature condition, introducing initial damage. Then, a monotonically increasing macro-strain is imposed to de **RVE** until it losses ellipticity.

The final configuration of the proposed **RVE** for different temperatures can be seen in Figure 4, showing a different failure mode for different temperatures. The homogenized stress-strain curves are plotted in Figure 5. It can be seen that the peak stress of the proposed constitutive model is reduced due to the damage induced by the temperature, and there is an increase in ductility. This results coincide with experimental analysis found in literature.

	Mortar	Aggregate	Interface
Young modulus E [MPa]	30800	37000	-
Poisson modulus	0.28	0.16	-
Critical tension σ_c [MPa]	6	-	3
Fracture energy G_c [N/mm]	0.14	-	0.070
Skeleton thermal expansion coefficient α_μ [1/°C]	$7.4e^{-6}$	$12.6e^{-6}$	-
Water thermal expansion coefficient α_w [1/°C]	$207e^{-6}$	-	-
Water porosity ϕ_w	0.16	-	-
Water Biot coefficient b_w	0.4073	-	-
Water Biot modulus M_w [MPa]	9400	-	-
Porous saturation degree S_w	0.5	-	-

Table 1: Properties for concrete.

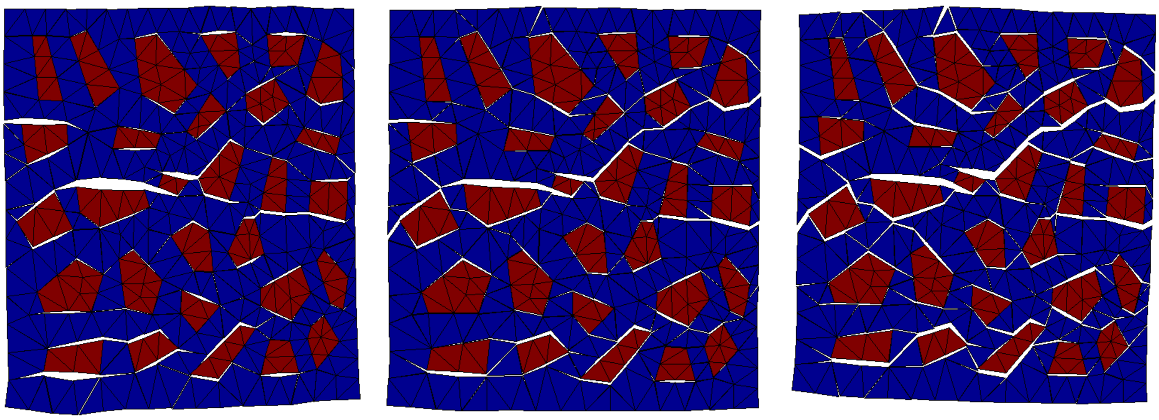

(a) Macro temperature $\theta = 0°C$. Displacement amplified $x500$.
(b) Macro temperature $\theta = 400°C$. Displacement amplified $x150$.
(c) Macro temperature $\theta = 700°C$. Displacement amplified $x100$.

Figure 4: Final configuration of the **RVE** for different temperatures and temperature gradient $\nabla_x^s \theta = (0, 0)$.

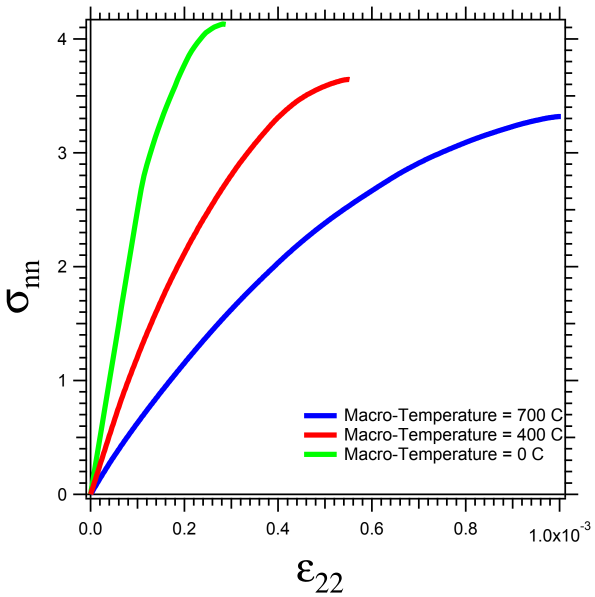

Figure 5: Homogenized stress versus strain curves for different temperatures.

The considered tensors of thermomechanical expansion for cement mortar and aggregates are

$$\boldsymbol{B}_{\mu}^{mortar} = \begin{bmatrix} 0.2072 \\ 0.2072 \\ 0 \end{bmatrix} \frac{MPa}{°C}, \qquad \boldsymbol{B}_{\mu}^{aggreg} = \begin{bmatrix} 0.3709 \\ 0.3709 \\ 0 \end{bmatrix} \frac{MPa}{°C}. \tag{44}$$

Using the homogenization procedure presented, the following homogenized thermal conductivity tensors for different sub-spaces are obtained

$$\boldsymbol{B}^{Taylor} = \begin{bmatrix} 0.2548 \\ 0.2548 \\ 0 \end{bmatrix} \frac{MPa}{^\circ C}, \qquad \boldsymbol{B}^{Traction} = \begin{bmatrix} 0.2507 \\ 0.2454 \\ 0.0164 \end{bmatrix} \frac{MPa}{^\circ C}. \tag{45}$$

6 Conclusions

A multi-scale model for thermo-poro-mechanic problems has been presented and discussed in this paper. Starting from a semi-concurrent formulation, the Helmholtz free energy of the mortar phase in the micro-scale is reformulated using the Biot theory for porous media to consider the effect of the pore pressure induced by the heat transfer through the material. Some numerical examples showing the homogenized response of a concrete like material are presented and discussed. The lost of resistance of the material due a temperature increasing has been numerically reproduced, and the final damage configuration is presented.

REFERENCES

[1] Blanco P.J., Giusti S.M. Thermomechanical Multiscale Constitutive Modeling: Accounting for Microstructural Thermal Effects, Journal of Elasticity: The Physical and Mathematical Science of Solids, 2013. Vol.111.

[2] López Rivarola F, Etse J.G. and Folino P. On Thermodynamic Consistency of Homogenization-based Multiscale Theories. ASME. J. Eng. Mater. Technol. 2017, doi:10.1115/1.4036243.

[3] Pignatelli Rossella. Modeling of degradation induced by alkali-silica reaction in concrete structures. Ph.D. Thesis, Politecnico di Milano.

[4] Labanda N.A., Giusti S.M. and Luccioni B.M. Meso-Scale Fracture Simulation using an augmented Lagrangian Approach. International Journal of Damage Mechanics, 2016. doi:10.1177/1056789516671092.